ACS Catalysis

Letter

pubs.acs.org/acscatalysis

Surface-Bound Ligands Modulate Chemoselectivity and Activity of a Bimetallic Nanoparticle Catalyst

Khanh B. Vu,[†,‡] Konstantin V. Bukhryakov,[†,‡] Dalaver H. Anjum,[§] and Valentin O. Rodionov*[,†]

[†]Division of Physical Sciences and Engineering and KAUST Catalysis Center, [§]KAUST Advanced Nanofabrication Imaging and Characterization Core Laboratory King Abdullah University of Science and Technology (KAUST), Thuwal 23955-6900, Kingdom of Saudi Arabia

Ⓢ *Supporting Information*

ABSTRACT: “Naked” metal nanoparticles (NPs) are thermodynamically and kinetically unstable in solution. Ligands, surfactants, or polymers, which adsorb at a particle’s surface, can be used to stabilize NPs; however, such a mode of stabilization is undesirable for catalytic applications because the adsorbates block the surface active sites. The catalytic activity and the stability of NPs are usually inversely correlated. Here, we describe an example of a bimetallic (PtFe) NP catalyst stabilized by carboxylate surface ligands that bind preferentially to one of the metals (Fe). NPs stabilized by fluorous ligands were found to be remarkably competent in catalyzing the hydrogenation of cinnamaldehyde; NPs stabilized by hydrocarbon ligands were significantly less active. The chain length of the fluorous ligands played a key role in determining the chemoselectivity of the FePt NP catalysts.

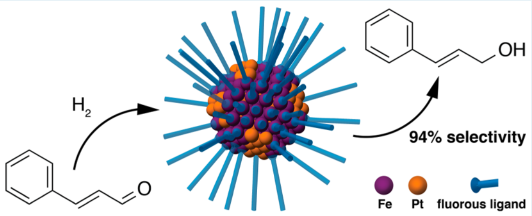

KEYWORDS: *cinnamaldehyde, selective hydrogenation, ligand effects, bimetallic nanoparticles, fluorous chemistry*

Transition metal nanoparticles (NPs) and nanoclusters are a privileged class of metal colloids.[1] Their high surface areas and the strong correspondence between particle sizes/shapes and surface chemistries make these species uniquely suited for applications in catalysis.[2−5] Small, catalytically active NPs are also some of the more unstable colloids because of their tendency to aggregate. To address this problem, NP catalysts are typically arrayed on solid supports,[1,6,7] which may also act as synergistic cocatalysts.[3,5,8]

NPs and metal clusters can also be stabilized and solubilized with the aid of surface adsorbates, which range from simple surfactants and amphiphilic copolymers to strongly binding/soft ligands, such as thiols.[9] Naturally, the adsorbate-stabilized NPs lose some or all of their catalytic prowess.[4,9] The metal surface accessibility is limited compared with “naked” NPs, and the catalytic sites are easily poisoned by thiols and amines. Before such NPs can be used as catalysts, a variety of harsh surface treatments are usually applied to remove the adsorbates.[9,10]

Here, we present an approach to dispersible, catalytically active, adsorbate-stabilized NPs. Our design is based on bimetallic NPs[7,11] consisting of metals that feature significantly different affinities toward a specific class of adsorbates. Thus, with judicious choice of metal composition and surface ligand chemistry, the particle aggregation could be prevented while the catalytic activity of the unprotected “islands” of the non-adsorbing metal could be preserved (Figure 1A). This approach was applied to FePt NPs[12] stabilized with perfluorinated carboxylic acids, which are expected to bind to Fe almost exclusively.[13] We were able to preserve the catalytic activity of Pt while gaining the capability for fluorous-biphasic recycling of

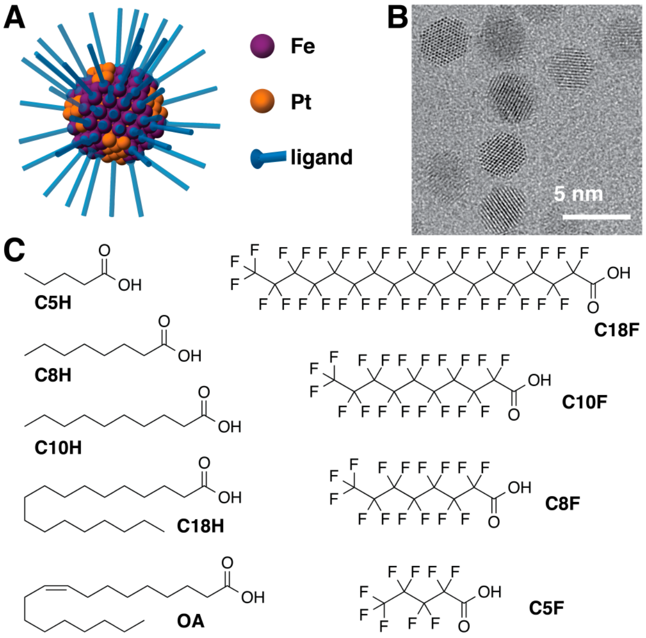

Figure 1. Selectively protected bimetallic NPs. (A) FePt NPs with ligand-free Pt sites. (B) TEM image of C10F−$Fe_{0.25}Pt_{0.75}$ NPs. (C) Carboxylic acid ligands used in this study.

Received: February 7, 2015
Revised: March 16, 2015
Published: March 17, 2015

DOI: 10.1021/acscatal.5b00262
ACS Catal. 2015, 5, 2529−2533

Table 1. Dependence of the Chemoselectivity and Activity of the FePt NP Catalysts on the Nature of Adsorbates[a]

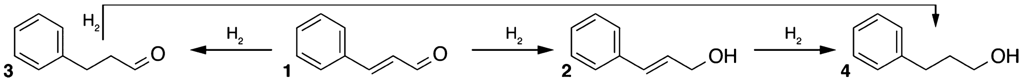

entry	catalyst	time, min	conversion, %[b]	**2**, %[b]	**3**, %[b]	**4**, %[b]	TON[c]	TOF, h^{-1}[c]
1	OA−Pt	60	14.9	16.2	55.8	28.0	18	18
2	C5H−$Fe_{0.25}Pt_{0.75}$	180	15.0	47.8	32.7	19.5	18	6
3	C10H−$Fe_{0.25}Pt_{0.75}$	180	17.8	52.0	31.3	16.8	22	7
4	C18H−$Fe_{0.25}Pt_{0.75}$	180	25.1	24.8	40.6	34.7	31	10
5	C5F−$Fe_{0.25}Pt_{0.75}$	90	12.0	72.1	18.6	9.3	15	10
6	C8F−$Fe_{0.25}Pt_{0.75}$	90	22.8	85.1	9.9	5.0	28	19
7	C10F−$Fe_{0.25}Pt_{0.75}$	90	43.1	91.8	4.4	3.8	53	35
8	C18F−$Fe_{0.25}Pt_{0.75}$	90	44.1	89.7	5.2	5.1	54	36
9	C10F−$Fe_{0.33}Pt_{0.67}$	60	71.1	94.0	1.5	4.5	87	87
10	C10F−$Fe_{0.13}Pt_{0.87}$	60	72.5	64.1	11.8	24.1	89	89

[a] Conditions: 0.1 mL of perfluorodecalin, 0.5 mL of *n*-hexane, H_2 (1 atm), 50 °C, cinnamaldehyde (0.16 mmol), catalyst (1.3×10^{-3} mmol Pt, 0.81 mol %). [b] Determined by NMR and GC/MS. [c] Turnover number (TON) and turnover frequency (TOF) calculated with respect to the overall Pt loading.[30]

the NP catalyst.[14] Serendipitously, we discovered that the perfluorinated adsorbates exert a significant influence over both the activity and chemoselectivity of the NP catalyst.

The FePt NPs used in this study were synthesized by the simultaneous decomposition of $Fe(CO)_5$ and reduction of $Pt(acac)_2$ in dioctyl ether by 1,2-hexadecanediol. In a departure from the previous reports of this procedure,[13,15] we used only oleic acid (OA) stabilizer, foregoing the use of oleylamine as the Pt capping ligand. We reasoned that in the absence of an amine, Pt "islands" will remain ligand-free. The NPs thus prepared were purified by centrifugation and redispersed in *n*-hexane. Although more prone to aggregation than the NPs stabilized by both amine and OA ligands, the OA-stabilized NPs were reasonably stable. Significant precipitation from hexane was typically observed only after several days to weeks, depending on the fraction of Fe, and we took care to perform all subsequent surface treatment or catalysis experiments with freshly prepared materials. To explore the mode of interaction of OA with the surfaces of pure Pt and FePt NPs, we obtained FTIR spectra of representative samples (Figure S13 A, SI). For C10F−$Fe_{0.25}Pt_{0.75}$ NPs, absorption bands at 2916, 2848, 1525, and 1399 cm^{-1} were observed. These bands are characteristic of OA adsorbed on a metal surface (Table S6, SI).[16] No such bands were observed for pure Pt NPs, indicating that the interaction of OA and Pt is weak, and any physisorbed OA is removed from the NP surfaces through simple washing/reprecipitation.

The Fe/Pt incorporation ratio could be tuned by changing the $Fe(CO)_5/Pt(acac)_2$ feed ratio. Because of the inevitable loss of the volatile carbonyl, the Fe/Pt ratio was determined by inductively coupled plasma optical emission spectroscopy. For convenience, the FePt NP materials will be designated Fe_xPt_y, where x and y are the molar fractions of the respective metals. Particles ranging from pure Pt to $Fe_{0.33}Pt_{0.67}$ have been prepared. To ascertain the nature of the metal packing in the NPs, they were characterized by powder X-ray diffraction (PXRD) (Figures S14 and S15, SI). The lattice constants obtained for the FePt materials through Rietveld refinement were smaller than that of Pt. This conclusion was further supported by selected area electron diffraction data (Figure S16 and Table S7, SI), suggesting a Pt-like alloy structure with randomly inserted Fe atoms.[17] The absence of peaks at 24° and 33°, which are characteristic of (001) and (110) lattice planes of the fct structure, indicated that $Fe_{0.13}Pt_{0.87}$, $Fe_{0.25}Pt_{0.75}$, and $Fe_{0.33}Pt_{0.77}$ feature disordered fcc structures with random distribution of Fe and Pt in the unit cell. This is unsurprising because the fcc-to-fct transformation in FePt NPs typically requires high temperature annealing.[18]

The size of OA-protected FePt NPs was in the range of 3.2−3.6 nm (Figure 1B, and SI Figures S6, S8, and S10), largely independent of the Fe/Pt ratio. Pure Pt nanoparticles prepared under the same conditions were ill-defined and aggregated (Figure S3). This confirms that OA has a poor affinity for the surface of Pt and is of limited use as a capping adsorbate in this case. Much larger FePt nanocrystals were obtained in the absence of OA, confirming the crucial role of the surface-bound OA in the stabilization of the FePt bimetallic particles during synthesis.[19]

The OA adsorbate could be conveniently exchanged for a range of other carboxylates, either perfluorinated or hydrocarbon. For the fluorous carboxylic acids, the exchange was performed in a mixture of dichloromethane and acetone. After incubation with the fluorous ligands, the NPs were extracted into perfluorodecalin (PFD). The material was purified from excess carboxylic acid by centrifugation and redispersed in PFD. The exchange procedure for the hydrocarbon carboxylic acids was more involved because the NPs could not be extracted into a fluorous solvent. Several centrifugation−redispersion steps were necessary to purify the catalyst from the excess adsorbate. Ligand exchange was not possible for OA−Pt NPs. As could be expected, these particles could not be redispersed in fluorous solvents after treatment with perfluorodecanoic acid. No fluorous acid could be detected on their surfaces by FTIR (Figure S13 B, SI). For convenience, the fluorous and hydrocarbon carboxylate ligands will be referred to as C*X*F and C*X*H respectively, where *X* is the length of the main carbon chain (Figure 1C). The corresponding NPs will be designated C*X*F−Fe_xPt_y and C*X*H−Fe_xPt_y.

The ligand exchange had no effect on the morphology of the FePt NPs, as observed by TEM (Figures S5 and S6, SI). However, both solubility and dispersion stability of the materials were significantly modified (Figure S1, SI). The effect was strongly dependent on both the nature of the carboxylic acid and the content of Fe in the NPs. Ligands with shorter carbon chains, such as C5F and C5H, predictably led to materials with poor colloidal stability. NPs stabilized with

DOI: 10.1021/acscatal.5b00262
ACS Catal. 2015, 5, 2529−2533

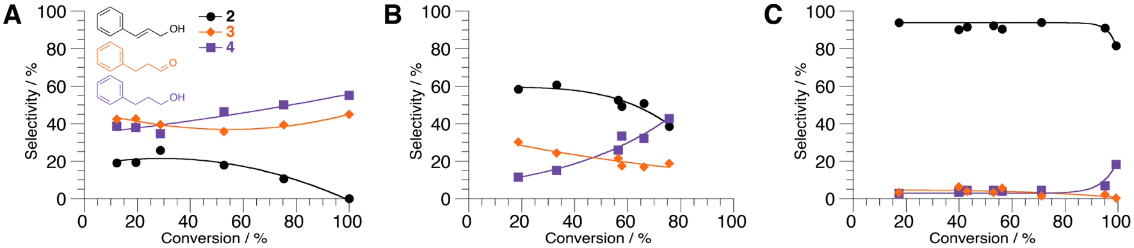

Figure 2. Product selectivity as a function of cinnamaldehyde conversion: (A) OA−Pt, (B) C10F−$Fe_{0.13}Pt_{0.87}$, and (C) C10F−$Fe_{0.33}Pt_{0.67}$. Conditions: 0.1 mL of perfluorodecalin; 0.5 mL of *n*-hexane; H_2 (1 atm); 50 °C; cinnamaldehyde (0.16 mmol); Pt loading (mol %), 19.2 (OA−Pt), 2.3 (C10F−$Fe_{0.13}Pt_{0.87}$), 0.62 (C10F−$Fe_{0.33}Pt_{0.67}$). The solid traces are provided for visual guidance only.

longer-chain adsorbates and Fe fractions over 0.25 were generally at least as stable as the parent OA-stabilized NPs. The attained stability was especially impressive for C10F and C18F ligands. The C10F−$Fe_{0.25}Pt_{0.75}$ NPs were stable in PFD solution for at least 2 weeks (Figure S2, SI); however, even the long-chain fluorous C10F was not sufficient to stabilize the low-Fe $Fe_{0.13}Pt_{0.87}$: although the NPs could be dispersed in PFD, significant precipitation was observed after 1 day. This observation provides further support for our selective adsorption hypothesis.

To explore the catalytic properties of the adsorbate-stabilized FePt NPs, we chose the hydrogenation of cinnamaldehyde as a model reaction. When catalyzed by Pt, this reaction leads to a range of products, with the hydrogenation of the C═C bond favored both thermodynamically (by ∼35 kJ·mol^{-1}) and kinetically.[20] The selectivity of the reaction can be adjusted in favor of C═O hydrogenation by performing it in the presence of metal salts,[21] under basic conditions,[22] or on hindered solid supports.[23] Bimetallic catalysts,[24] especially CoPt[25] and FePt[26] at high pressure of H_2,[27] can be C═O-selective. The selectivity can also be imparted by sterically hindered capping ligands.[28] A recent report describes a C═O-selective hydrogenation achieved through specific noncovalent interactions between cinnamaldehyde and the surface capping ligands.[29]

We performed cinnamaldehyde hydrogenations in a mixture of hexane and perfluorodecalin at 50 °C and 1 atm of H_2. Because this solvent mixture phase-separates at lower temperatures, all the C*X*F-protected NP catalysts could be conveniently recovered and recycled simply by separating the fluorous phase containing the NPs. The colloidal stability of the catalysts stabilized by longer-chain (>C10) C*X*F ligands was exceptional. The phase mixing/separation could be repeated at least 10 times for C18F- $Fe_{0.25}Pt_{0.75}$ without inducing NP aggregation.

For all the FePt NP catalysts, the selectivity and reactivity could be readily tuned by changing the length and nature of the carboxylic acid chains and the Fe content of the catalyst (Table 1 and Figure 2). The parent OA−Pt catalyst, while prone to aggregation, was active under the mild conditions employed, converting 14.9% of cinnamaldehyde in 1 h. As expected, 3-phenylpropanal **3** and 3-phenyl-1-propanol **4** were the major products (Table 1, entry 1). The C*X*H−$Fe_{0.25}Pt_{0.75}$ catalysts were somewhat less active than pure Pt (Table 1, entries 2−4). The chemoselectivity of these catalysts was shifted in favor of the C═O hydrogenation product. This modest change in chemoselectivity was in line with what could generally be expected from a FePt catalyst[26] and attributable to the surface ensemble effect produced through Fe substitution on fcc-packed Pt surface. The NPs stabilized with C18H, the longest chain in the series, were both more active and less selective than either the C5H- or C10H- stabilized catalysts. This suggests that the steric effect of the surface C*X*H ligands and the surface ensemble effect may be antagonistic.

The change from hydrocarbon-based to fluorous adsorbates effected a dramatic change in the activity and selectivity of the FePt catalysts. All the C*X*F-capped NPs showed an extremely high preference for C═O hydrogenation (Table 1, Entries 5−10). It is important to note that the rate of the hydrogenation was markedly accelerated by the longer-chain C8F−C18F adsorbates (Table 1, entries 6−10). Quantitative conversion of cinnamaldehyde could be achieved over the C10F−$Fe_{0.33}Pt_{0.67}$ catalyst after ∼1.3 h (Figure S29, SI). Both the activity and selectivity of the C*X*F-capped catalysts were strongly correlated with the Fe content of the NPs (Table 1, entries 7, 9, and 10). The relatively low-Fe C10F−$Fe_{0.13}Pt_{0.87}$ catalyst was markedly less selective than either C10F−$Fe_{0.25}Pt_{0.75}$ or C10F−$Fe_{0.33}Pt_{0.67}$.

Next, we explored the dependence of product selectivity on the degree of conversion for a number of NP catalysts (Figure 2). The pure Pt catalyst was not especially selective. 3-Phenylpropanal and the secondary product 3-phenyl-1-propanol were dominant, whereas cinnamyl alcohol all but disappeared from the reaction mixture at higher conversions (Figure 2A). For C10F−$Fe_{0.13}Pt_{0.87}$, the selectivity was shifted markedly in favor of cinnamyl alcohol (Figure 2B). Another notable change compared with the pure Pt was the decrease in abundance of 3-phenylpropanol, especially at lower conversions. The change in selectivity was even more dramatic for C10F−$Fe_{0.33}Pt_{0.67}$ (Figure 2C). This catalyst formed cinnamyl alcohol almost exclusively until a very high degree of conversion (>90%). Only then could a minor amount of 3-phenyl-1-propanol be detected in the reaction mixture, indicating that this product is formed through slow hydrogenation of cinnamyl alcohol. Notably, this remarkable improvement in selectivity was achieved concomitantly with an increase in the reaction rate and turnover frequency.

As expected, the FePt catalysts were readily poisoned by either amines or thiols (section 3, SI). Addition of (perfluorooctyl)propylamine to C10F−$Fe_{0.25}Pt_{0.75}$ led to a substantial reaction rate decrease (by half), and an analogous thiol completely deactivated the catalyst. Because both amines and thiols have a high affinity for Pt surfaces, we believe the poisoning affects only the Pt islands that are free from the carboxylic acid adsorbate.

The dramatic rate and selectivity differences between the FePt catalysts can be readily explained by considering the steric and nanoenvironment effects exerted by the surface-bound ligands. The adsorbed carboxylic acids are expected to provide a degree of site isolation to the Pt sites on the NP surface. Longer-chain ligands constrain the geometry around these sites, permitting only the head-on approach of the substrate. With a sufficient density of the surface ligands, a sideways approach of cinnamaldehyde to Pt needed for the C=C hydrogenation can be completely prevented. Thus, a preference for the C=O hydrogenation is realized.[29] The perfluorinated carboxylic acids are more rigid/rodlike than their hydrocarbon counterparts.[31] Thus, the geometric confinement effect is much more pronounced for the CXF-protected NPs. As the carboxylate ligands bind preferentially to Fe, the density of the surface-bound chains and the degree of catalytic site confinement increase with a rise in the Fe content. Thus, catalysts containing more Fe are more C=O-selective. We also expect that the "everything-phobic" fluorous ligands[32] surrounding the active sites will facilitate the desorption of the inactive reaction intermediates[33] and discourage the unproductive binding of products and substrates.

In conclusion, we explored the catalytic activity of a range of FePt bimetallic NPs stabilized by carboxylate ligands. These ligands have a high affinity for only one of the metals (Fe). The NPs stabilized by fluorous ligands were remarkably active in catalyzing the hydrogenation of cinnamaldehyde. The chemoselectivity of the catalysis was significantly altered with respect to the parent Pt catalyst. Longer-chain fluorous carboxylic acid ligands shifted the selectivity almost entirely in favor of C=O hydrogenation, with a concomitant *increase* in the reaction rate. These effects could be readily explained by considering the isolation/crowding of the Pt active sites by the rigid fluorous ligands. The fluorous-stabilized bimetallic NPs had excellent colloidal stability and were readily recyclable. Investigations of other bimetallic NP catalysts selectively functionalized with surface adsorbates are under way in our laboratories.

■ ASSOCIATED CONTENT

Ⓢ Supporting Information

The following files are available free of charge on the ACS Publications website at DOI: 10.1021/acscatal.5b00262.

Additional experimental details and characterization (TEM, EDS, SAED, PXRD, ^{1}H NMR, GC/MS chromatograms) (PDF)

Video of catalyst separation/recycling (AVI)

■ AUTHOR INFORMATION

Corresponding Author

*Phone: +966-12-8084592. E-mail: valentin.rodionov@kaust.edu.sa.

Author Contributions

‡K.B.V. and K.V.B. contributed equally.

Notes

The authors declare no competing financial interest.

■ ACKNOWLEDGMENTS

The authors are grateful to Prof. J.-M. Basset for helpful discussions. This research was supported by King Abdullah University of Science and Technology.

■ REFERENCES

(1) Roucoux, A.; Schulz, J.; Patin, H. *Chem. Rev.* **2002**, *102*, 3757–3778.

(2) (a) Bell, A. T. *Science* **2003**, *299*, 1688–1691. (b) Haruta, M. *Chem. Rec.* **2003**, *3*, 75–87.

(3) Jia, C.-J.; Schuth, F. *Phys. Chem. Chem. Phys.* **2011**, *13*, 2457–2487.

(4) Narayanan, R.; El-Sayed, M. A. *J. Phys. Chem. B* **2005**, *109*, 12663–12676.

(5) Astruc, D.; Lu, F.; Aranzaes, J. R. *Angew. Chem., Int. Ed.* **2005**, *44*, 7852–7872.

(6) White, R. J.; Luque, R.; Budarin, V. L.; Clark, J. H.; Macquarrie, D. J. *Chem. Soc. Rev.* **2009**, *38*, 481–494.

(7) Thomas, J. M.; Johnson, B. F. G.; Raja, R.; Sankar, G.; Midgley, P. A. *Acc. Chem. Res.* **2002**, *36*, 20–30.

(8) (a) Králik, M.; Biffis, A. *J. Mol. Catal. A: Chem.* **2001**, *177*, 113–138. (b) Green, I. X.; Tang, W.; Neurock, M.; Yates, J. T. *Acc. Chem. Res.* **2013**, *47*, 805–815. (c) McEntee, M.; Tang, W.; Neurock, M.; Yates, J. T. *J. Am. Chem. Soc.* **2014**, *136*, 5116–5120. (d) Corma, A.; Garcia, H. *Chem. Soc. Rev.* **2008**, *37*, 2096–2126.

(9) Niu, Z.; Li, Y. *Chem. Mater.* **2013**, *26*, 72–83.

(10) (a) Li, D.; Wang, C.; Tripkovic, D.; Sun, S.; Markovic, N. M.; Stamenkovic, V. R. *ACS Catal.* **2012**, *2*, 1358–1362. (b) Ansar, S. M.; Ameer, F. S.; Hu, W.; Zou, S.; Pittman, C. U.; Zhang, D. *Nano Lett.* **2013**, *13*, 1226–1229. (c) Crespo-Quesada, M.; Andanson, J.-M.; Yarulin, A.; Lim, B.; Xia, Y.; Kiwi-Minsker, L. *Langmuir* **2011**, *27*, 7909–7916. (d) Solla-Gullon, J.; Montiel, V.; Aldaz, A.; Clavilier, J. *J. Electrochem. Soc.* **2003**, *150*, E104–E109.

(11) Toshima, N.; Yonezawa, T. *New J. Chem.* **1998**, *22*, 1179–1201.

(12) Sun, S. H. *Adv. Mater.* **2006**, *18*, 393–403.

(13) Ofir, Y.; Samanta, B.; Arumugam, P.; Rotello, V. M. *Adv. Mater.* **2007**, *19*, 4075–4079.

(14) (a) Horváth, I. T.; Rábai, J. *Science* **1994**, *266*, 72–75. (b) Chechik, V.; Crooks, R. M. *J. Am. Chem. Soc.* **2000**, *122*, 1243–1244.

(15) Sun, S. H.; Murray, C. B.; Weller, D.; Folks, L.; Moser, A. *Science* **2000**, *287*, 1989–1992.

(16) (a) Wu, N. Q.; Fu, L.; Su, M.; Aslam, M.; Wong, K. C.; Dravid, V. P. *Nano Lett.* **2004**, *4*, 383–386. (b) Klokkenburg, M.; Hilhorst, J.; Erne, B. H. *Vib. Spectrosc.* **2007**, *43*, 243–248.

(17) Howard, L. E. M.; Nguyen, H. L.; Giblin, S. R.; Tanner, B. K.; Terry, I.; Hughes, A. K.; Evans, J. S. O. *J. Am. Chem. Soc.* **2005**, *127*, 10140–10141.

(18) Nguyen, H. L.; Howard, L. E. M.; Stinton, G. W.; Giblin, S. R.; Tanner, B. K.; Terry, I.; Hughes, A. K.; Ross, I. M.; Serres, A.; Evans, J. S. O. *Chem. Mater.* **2006**, *18*, 6414–6424.

(19) Samia, A. C. S.; Schlueter, J. A.; Jiang, J. S.; Bader, S. D.; Qin, C.-J.; Lin, X.-M. *Chem. Mater.* **2006**, *18*, 5203–5212.

(20) (a) Gallezot, P.; Richard, D. *Catal. Rev. Sci. Eng.* **1998**, *40*, 81–126. (b) Yuan, Y.; Yao, S.; Wang, M.; Lou, S.; Yan, N. *Curr. Org. Chem.* **2013**, *17*, 400–413. (c) Mohr, C.; Claus, P. *Sci. Prog.* **2001**, *84*, 311–334.

(21) (a) Tuley, W. F.; Adams, R. *J. Am. Chem. Soc.* **1925**, *47*, 3061–3068. (b) Galvagno, S.; Donato, A.; Neri, G.; Pietropaolo, R.; Pietropaolo, D. *J. Mol. Catal.* **1989**, *49*, 223–232.

(22) Bhogeswararao, S.; Srinivas, D. *J. Catal.* **2012**, *285*, 31–40.

(23) (a) Blackmond, D. G.; Oukaci, R.; Blanc, B.; Gallezot, P. *J. Catal.* **1991**, *131*, 401–411. (b) Guo, Z.; Xiao, C.; Maligal-Ganesh, R. V.; Zhou, L.; Goh, T. W.; Li, X.; Tesfagaber, D.; Thiel, A.; Huang, W. *ACS Catal.* **2014**, *4*, 1340–1348.

(24) Qi, X.; Axet, M. R.; Philippot, K.; Lecante, P.; Serp, P. *Dalton Trans.* **2014**, *43*, 9283–9295.

(25) Tsang, S. C.; Cailuo, N.; Oduro, W.; Kong, A. T. S.; Clifton, L.; Yu, K. M. K.; Thiebaut, B.; Cookson, J.; Bishop, P. *ACS Nano* **2008**, *2*, 2547–2553.

(26) da Silva, A. B.; Jordão, E.; Mendes, M. J.; Fouilloux, P. *Appl. Catal., A* **1997**, *148*, 253–264.

(27) (a) Goupil, D.; Fouilloux, P.; Maurel, R. *React. Kinet. Catal. Lett.* **1987**, *35*, 185–193. (b) Liu, Z.; Tan, X.; Li, J.; Lv, C. *New J. Chem.* **2013**, *37*, 1350–1357.

(28) Wu, B. H.; Huang, H. Q.; Yang, J.; Zheng, N. F.; Fu, G. *Angew. Chem., Int. Ed.* **2012**, *51*, 3440–3443.

(29) Kahsar, K. R.; Schwartz, D. K.; Medlin, J. W. *J. Am. Chem. Soc.* **2013**, *136*, 520–526.

(30) Umpierre, A. P.; de Jesús, E.; Dupont, J. *ChemCatChem* **2011**, *3*, 1413–1418.

(31) Eaton, D. F.; Smart, B. E. *J. Am. Chem. Soc.* **1990**, *112*, 2821–2823.
(32) Kirsch, P. *Modern Fluoroorganic Chemistry: Synthesis, Reactivity, Applications*; Wiley-VCH: Weinheim, 2005; pp 1–23.
(33) Wang, H.; Krier, J. M.; Zhu, Z.; Melaet, G.; Wang, Y.; Kennedy, G.; Alayoglu, S.; An, K.; Somorjai, G. A. *ACS Catal.* **2013**, *3*, 2371–2375.